Inorg. Chem. **2004**, *43*, 5486–5488

Linear Ni^{II}–Mn^{III}_2–Ni^{II} Tetramers: An Oligomeric Component of the $Mn^{III}_2Ni^{II}$ Single-Chain Magnets

Hitoshi Miyasaka,*[†,‡] Tomohiro Nezu,[†] Kunihisa Sugimoto,[§] Ken-ichi Sugiura,[†] Masahiro Yamashita,[†,||] and Rodolphe Clérac[⊥]

Department of Chemistry, Graduate School of Science, Tokyo Metropolitan University, 1-1 Minami-Ohsawa, Hachioji, Tokyo 192-0397, Japan, PRESTO, Japan Science and Technology Agency, 4-1-8 Honcho, Kawaguchi, Saitama 332-0012, Japan, X-ray Research Laboratory, Rigaku Co. Ltd., 3-9-12 Matsubara-cho, Akishima, Tokyo 196-8666, Japan, CREST, Japan Science and Technology Agency, 4-1-8 Honcho, Kawaguchi, Saitama 332-0012, Japan, and Centre de Recherche Paul Pascal, CNRS UPR 8641, 115 avenue du Dr. A. Schweitzer, 33600 Pessac, France

Received April 28, 2004

Heterometallic linear tetramers $[Mn(5\text{-R-saltmen})Ni(pao)(bpy)_2]_2(ClO_4)_4$ (5-R-saltmen^{2-} = *N*,*N*′-1,1,2,2-tetramethylethylene bis(5-R-salicylideneiminate); pao$^-$ = pyridine-2-aldoximate; bpy = 2,2′-bipyridine, R = H, **1**; Cl, **2**; Br, **3**; MeO, **4**) have been synthesized and structurally characterized. These compounds exhibit a [Ni^{II}–NO–Mn^{III}–$(O)_2$–Mn^{III}–ON–Ni^{II}] skeleton where –ON– is an oximate bridge between Mn^{III} and Ni^{II} ions and –$(O)_2$– is a bi-phenolate bridge between Mn^{III} ions. These tetramers can be seen as oligomeric units of the heterometallic Mn^{III}_2–Ni^{II} chain observed in a family of single-chain magnets (Clérac, R.; Miyasaka, H.; Yamashita, M.; Coulon, C. *J. Am. Chem. Soc.* **2002**, *124*, 12837. Miyasaka, H.; Clérac, R.; Mizushima, K.; Sugiura, K.; Yamashita, M.; Wernsdorfer, W.; Coulon, C. *Inorg. Chem.* **2003**, *42*, 8203.). Magnetic measurements on these tetramers confirm the nature of the magnetic interactions reported for the Mn^{III}_2–Ni^{II} chains: a strong antiferromagnetic Mn^{III}/Ni^{II} coupling via the oximate bridge (J_{Ni-Mn} ranges from –23.7 to –26.1 K) and a weak ferromagnetic Mn^{III}/Mn^{III} coupling through the bi-phenolate bridge (J_{Mn-Mn} ranges from +0.4 to +0.9 K). These magnetic interactions lead to tetramers with an $S = 2$ ground state.

In the field of molecule-based magnetism, the most recent success has been the synthesis of single-chain magnets (SCMs), i.e., one-dimensional materials with Glauber-like[1] slow relaxation of their magnetization.[2−4] In these paramagnetic materials, short-range order is more and more important upon lowering the temperature until $T = 0$ K, the critical temperature for any 1D system. In agreement with the pioneering work of Glauber,[1] the relaxation time is exponentially enhanced at low temperatures, and this relaxation process can take years as seen in single-molecule magnets.[5] Therefore, this type of material can be considered as a magnet even if no long-range order is stabilized like in classical bulk magnets. Our group published two years ago[3a] a prototype example of the anisotropic ferromagnetically coupled 1D system as described by Glauber. On the basis of this genuine compound, series of SCMs containing Mn^{III}/Ni^{II} heterometallic chains have been obtained: $[Mn_2(saltmen)_2Ni(pao)_2(L^1)_2](X)_2$ (L^1 = pyridine, 4-picoline, 4-*tert*-butylpyridine, *N*-methylimidazole; X = ClO_4^-, BF_4^-, PF_6^-, ReO_4^-).[3b] The $S_T = 3$ repeating unit along these chains is based on the [−Mn^{III}−ON−Ni^{II}−NO−Mn^{III}−] motif and strong antiferromagnetic coupling between Mn^{III} and Ni^{II} via the oximate (−NO−) bridge ($-25 < J_{Mn-Ni}/k_B < -20$ K). A quasi-Ising chain is obtained by ferromagnetic coupling, J_{Mn-Mn}, of these anisotropic trimers through the bi-phenolate (−O_2−) bridge ($0.6 < J_{Mn-Mn}/k_B < 0.9$ K). In this paper, we report the deliberate design of new Ni_2Mn_2 tetramers, $[Mn(5\text{-R-saltmen})Ni(pao)(bpy)_2]_2(ClO_4)_4$ (R = H, **1**; Cl, **2**; Br, **3**; MeO, **4**) (Chart 1), reminiscent of the structure found in the SCMs described above.

* To whom correspondence should be addressed. E-mail: miyasaka@comp.metro-u.ac.jp. Fax: (+81) 426-77-2525.
† Tokyo Metropolitan University.
‡ PRESTO, JST.
§ Rigaku Co. Ltd.
|| CREST, JST.
⊥ CRPP.

(1) Glauber, R. J. *J. Math. Phys.* **1963**, *4*, 294. Susuki, M.; Kubo, R. *J. Phys. Soc. Jpn.* **1968**, *24*, 51.
(2) (a) Caneschi, A.; Gatteschi, D.; Lalioti, N.; Sangregorio, C.; Sessoli, R.; Venturi, G.; Vindigni, A.; Rettori, A.; Pini, M. G.; Novak, M. A. *Angew. Chem., Int. Ed.* **2001**, *40*, 1760. (b) Caneschi, A.; Gatteschi, D.; Lalioti, N.; Sangregorio, C.; Sessoli, R.; Venturi, G.; Vindigni, A.; Rettori, A.; Pini, M. G.; Novak, M. A. *Europhys. Lett.* **2002**, *58*, 771.
(3) (a) Clérac, R.; Miyasaka, H.; Yamashita, M.; Coulon, C. *J. Am. Chem. Soc.* **2002**, *124*, 12837. (b) Miyasaka, H.; Clérac, R.; Mizushima, K.; Sugiura, K.; Yamashita, M.; Wernsdorfer, W.; Coulon, C. *Inorg. Chem.* **2003**, 42, 8203. (c) Coulon, C.; Clérac, R.; Lecren, L.; Wernsdorfer, W.; Miyasaka, H. *Phys. Rev. B* **2004**, *69*, 132408.
(4) (a) Lescouëzec, R.; Vaissermann, J.; Ruiz-Pérez, C.; Lloret, F.; Carrasco, R.; Julve, M.; Verdaguer, M.; Dromzee, Y.; Gatteschi, D.; Wernsdorfer, W. *Angew. Chem., Int. Ed.* **2003**, *42*, 1483. (b) Liu, T.; Fu, D.; Gao, S.; Zhang, Y.; Sun, H.; Su, G.; Liu, Y. *J. Am. Chem. Soc.* **2003**, *125*, 13976.
(5) (a) Christou, G.; Gatteschi, D.; Hendrickson, D. N.; Sessoli, R. *MRS Bull.* **2000**, *25*, 66. (b) Gatteshi, D.; Sessoli, R. *Angew. Chem., Int. Ed.* **2003**, *42*, 268.

10.1021/ic049457q CCC: $27.50
Published on Web 07/31/2004

Chart 1

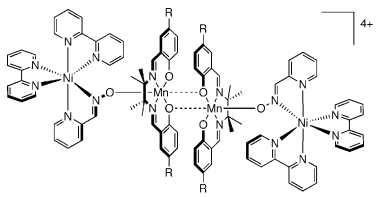

[Mn(5-R-saltmen)Ni(pao)(bpy)$_2$]$_2$(ClO$_4$)$_4$
R = H, **1**; Cl, **2**; Br, **3**; MeO, **4**

Whereas Ni(pao)$_2$(L^1)$_2$ precursors acted as bridging metalloligands in the SCM series,[3,6] the [Ni(pao)(bpy)$_2$]$^+$ building block was designed to act as a terminal ligand (unidentate metalloligand) by using one pao$^-$ and two bpy ligands.[7] As expected, the assembly reaction of this new precursor with [Mn$_2$(5-R-saltmen)$_2$(H$_2$O)$_2$](ClO$_4$)$_2$ in a molar ratio of 2:1 and in methanol/water medium produced linear tetramers **1**−**4** independent of the 5-R substituent.[8] Compounds **2**−**4** are isostructural and crystallized in the monoclinic space group $P2_1/n$.[9] The recurrent tetranuclear structure is shown for **2** in Figure 1. Selected bond distances and angles of the bridging structure are summarized in Table 1. The linear-type tetramer has an inversion center in the midpoint of the [Mn$_2$(5-R-saltmen)$_2$]$^{2+}$ dimeric core. This centrosymmetry ensures the presence of the Δ and Λ isomer forms of the terminal [Ni(pao)(bpy)$_2$]$^+$ moieties. The Ni coordination sphere adopts a slightly distorted octahedral geometry surrounded by two bpy and one pao$^-$ ligands with the average Ni−N distance of 2.07 Å. The Mn−O−N angles fall in the range 129−132°, close to those observed in the [Mn$_2$(saltmen)$_2$Ni(pao)$_2$(L^1)$_2$](A)$_2$ family.[3] Whereas the Mn−O$_{oximate}$ bond distance is about 2.077(3) Å in **2** and **3**, this bond is slightly longer in **4** (2.106(3) Å). The reverse trend is found for Mn−O(1*) bond distances (Table 1). Among these tetramers, even if the out-of-plane dimeric core is globally similar, these small bond distance and angle variations are probably due to the effect of the 5-R group. Mn ions display a strongly distorted octahedral geometry surrounded in equatorial sites by the tetradentate 5-R-saltmen^{2-} ligand and occupied in apical positions by oxygen atoms from the oximate group and neighboring Mn(5-R-saltmen) moiety. The apical Mn−O bond distances are significantly longer than the equatorial ones as expected for Jahn−Teller distorted Mn^{III} ion.

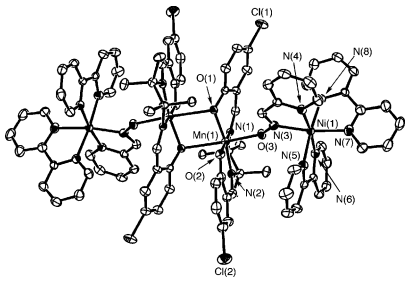

Figure 1. ORTEP view of tetramer **2** (50% probability ellipsoid).

Table 1. Selected Bond Distances and Angles in Bridging Structures of **2**−**4**

	2	**3**	**4**
Ni(1)−N(3)	2.044(3)	2.042(4)	2.031(4)
Mn(1)−O(3)[a]	2.075(3)	2.080(3)	2.106(3)
Mn(1)−O(1)	1.925(3)	1.929(3)	1.934(3)
Mn(1)−O(1*)	2.492(3)	2.493(3)	2.416(3)
N(3)−O(3)[a]	1.318(4)	1.307(5)	1.332(5)
Mn(1)···Mn(1*)	3.4248(8)	3.4286(8)	3.3826(9)
Ni(1)−N(3)−O(3)[a]	124.0(2)	124.6(3)	123.0(2)
Mn(1)−O(3)−N(3)[a]	131.1(2)	132.4(2)	129.2(2)
Mn(1)−O(1)−Mn(1*)	100.9(1)	100.9(1)	101.5(1)
O(1)−Mn(1)−O(1*)	79.1(1)	79.1(1)	78.5(1)

[a] O(3) corresponds to O(5) in **3**. Symmetry operation (*): $-x, -y, -z$.

Direct current magnetic susceptibility on polycrystalline samples of **1**−**4** was studied between 1.82 and 300 K at 0.1 T. The whole magnetic behavior has been found very similar along this series, which, despite the lack of crystal structure for **1**, supports clearly that the tetramer motif is also present in **1**. As a representative example, the magnetic data will be shown for **1** in Figure 2 (data for **2**−**4** available in Supporting Information). Above 150 K, the susceptibility roughly obeys a Curie−Weiss law with $C = 8.8$ emu·K·mol^{-1}, $\theta = -72$ K for **1**, $C = 8.8$ emu·K·mol^{-1}, $\theta = -84$ K for **2**, $C = 8.7$

(6) (a) Miyasaka, H.; Mizushima, K.; Sugiura, K.; Yamashita, M. *Synth. Met.* **2003** *137*, 1245. (b) Miyasaka, H.; Furukawa, S.; Yanagida, S.; Sugiura, K.; Yamashita, M. *Inorg. Chim. Acta* **2004**, *33*, 578.

(7) Synthesis of [Ni(Hpao)(bpy)$_2$](ClO$_4$)$_2$·0.5H$_2$O: a solution of water/ethanol (4:1, 20 mL) containing pyridine-2-aldoxime (244 mg, 2 mmol) was added to an aquous solution (20 mL) of [Ni(bpy)$_2$(H$_2$O)$_2$](ClO$_4$)$_2$·0.5EtOH (1.258 g, 2 mmol). After several minutes of stirring at room temperature, a pale brown precipitate formed out the brown solution. After further stirring for 30 min, the precipitate was filtered and dried in vacuo. Yield 61% (860 mg). Anal. Calcd for $C_{26}H_{23}Cl_2N_6NiO_{9.5}$: C, 44.54; H, 3.31; N, 11.99. Found: C, 44.46; H, 3.32; N, 11.87. IR (KBr): ν (bpy C═N), 1566, 1575 cm^{-1}; ν (ClO$_4$), 1092 cm^{-1}: ν (Schiff C═N), 1603 cm^{-1}.

(8) Syntheses of **1**−**4**: The whole series of compounds can be synthesized in a similar manner. Therefore, only the synthesis **1** will be described here. To a methanol solution (20 mL) of [Ni(Hpao)(bpy)$_2$](ClO$_4$)$_2$·0.5H$_2$O (280 mg, 0.4 mmol) was added solid NaOH (80 mg, 2 mmol) to generate [Ni(pao)(bpy)$_2$]$^+$ species. The mixture was added to a methanol solution (30 mL) of [Mn(saltmen)(H$_2$O)]ClO$_4$ (198 mg, 0.4 mmol). After stirring for 30 min, the obtained brown solution was filtered and allowed to stand for 3 days to form dark brown microcrystals of **1**·MeOH·2H$_2$O (yield: 51%, 225 mg). Anal. Calcd for $C_{93}H_{94}Cl_4Mn_2N_{16}Ni_2O_{25}$: C, 50.66; H, 4.30; N, 10.16. Found: C, 50.36; H, 4.10; N, 10.30. IR (KBr): ν (C═N), 1603 cm^{-1}; ν (ClO$_4$), 1090 cm^{-1}. For **2**: yield 62%. Anal. Calcd for $C_{92}H_{82}Cl_8Mn_2N_{16}Ni_2O_{22}$: C, 48.58; H, 3.63; N, 9.85. Found: C, 48.49; H, 3.67; N, 9.85. IR (KBr): ν (C═N), 1605 cm^{-1}; ν (ClO$_4$), 1088 cm^{-1}. For **3**: yield 50%. Anal. Calcd for $C_{92}H_{82}Br_4Cl_4Mn_2N_{16}Ni_2O_{22}$: C, 45.06; H, 3.37; N, 9.14. Found: C, 44.77; H, 3.41; N, 9.10. IR (KBr): ν (C═N), 1605 cm^{-1}; ν (ClO$_4$), 1090 cm^{-1}. For **4**: yield 48%. Anal. Calcd for $C_{96}H_{94}Cl_4Mn_2N_{16}Ni_2O_{26}$: C, 51.09; H, 4.20; N, 9.93. Found: C, 50.86; H, 4.22; N, 9.97. IR (KBr): ν (C═N), 1603 cm^{-1}; ν (ClO$_4$), 1088 cm^{-1}.

(9) Crystal data for **2**: $C_{92}H_{82}N_{16}O_{22}Cl_8Mn_2Ni_2$, fw = 2274.65, monoclinic $P2_1/n$ (No. 14), $T = 150 \pm 1$ K, $a = 12.796(6)$ Å, $b = 19.069(9)$ Å, $c = 20.225(9)$ Å, $\beta = 94.706(2)°$, $V = 4918.5(39)$ Å^3, $Z = 2$, $D_{calc} = 1.536$ g·cm^{-3}, $F_{000} = 2328.00$, μ(Mo Kα) = 9.24 cm^{-1}, final R1 = 0.053 ($I > 2.00\sigma(I)$), $R = 0.075$ (all data), wR2 = 0.154 (all data), GOF = 1.005, $\rho_{max} = 1.16$ e$^-$/Å^3, $\rho_{min} = -0.80$ e$^-$/Å^3. Crystal data for **3**: $C_{92}H_{82}N_{16}O_{22}Cl_4Mn_2Ni_2Br_4$, fw = 2452.46, monoclinic $P2_1/n$ (No. 14), $T = 150 \pm 1$ K, $a = 12.8276(3)$ Å, $b = 19.0950(4)$ Å, $c = 20.3129(5)$ Å, $\beta = 94.1396(12)°$, $V = 4962.5(2)$ Å^3, $Z = 2$, $D_{calc} = 1.641$ g·cm^{-3}, $F_{000} = 2472.00$, μ(Mo Kα) = 24.24 cm^{-1}, final R1 = 0.050 ($I > 2.00\sigma(I)$), $R = 0.062$ (all data), wR2 = 0.150 (all data), GOF = 1.000, $\rho_{max} = 2.05$ e$^-$/Å^3, $\rho_{min} = -1.09$ e$^-$/Å^3. Crystal data for **4**: $C_{96}H_{94}N_{16}O_{26}Cl_4Mn_2Ni_2$, fw = 2256.98, monoclinic $P2_1/n$ (No. 14), $T = 150 \pm 1$ K, $a = 13.206(5)$ Å, $b = 18.707(8)$ Å, $c = 20.103(8)$ Å, $\beta = 96.578(6)°$, $V = 4933.5(34)$ Å^3, $Z = 2$, $D_{calc} = 1.519$ g·cm^{-3}, $F_{000} = 2328.00$, μ(Mo Kα) = 8.19 cm^{-1}, final R1 = 0.056 ($I > 2.00\sigma(I)$), $R = 0.092$ (all data), wR2 = 0.108 (all data), GOF = 1.015, $\rho_{max} = 0.89$ e$^-$/Å^3, $\rho_{min} = -0.98$ e$^-$/Å^3.

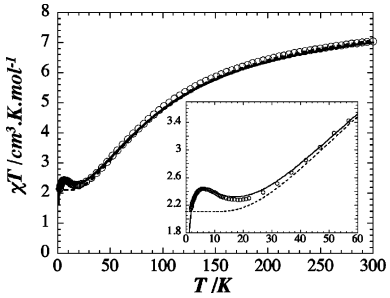

Figure 2. χT vs T plot of **1** at 0.1 T. The solid and dashed lines represent the simulation with the $Ni^{II}-Mn^{III}-Mn^{III}-Ni^{II}$ tetramer (and intermolecular interactions) and $Mn^{III}-Ni^{II}$ dimer models, respectively (see text). Inset: close-up view of the low temperature region.

Table 2. Magnetic Parameters Obtained from Simulation of χT Using a Ni−Mn−Mn−Ni Tetramer Model with Intermolecular Interactions (See Text)

compd	g_{av}	J_{Ni-Mn}/k_B [K]	J_{Mn-Mn}/k_B [K]	zJ/k_B [K]
1	2.04(1)	−23.7(2)	+0.90(5)	−0.23(2)
2	2.04(1)	−26.1(2)	+0.70(5)	−0.20(2)
3	2.04(1)	−25.1(2)	+0.80(5)	−0.23(2)
4	1.96(1)	−24.4(2)	+0.40(5)	−0.18(2)

emu·K·mol^{-1}, $\theta = -76$ K for **3**, and $C = 8.0$ emu·K·mol^{-1}, $\theta = -73$ K for **4**. Curie constants are in good agreement with the expected values for 2 Mn^{III} and 2 Ni^{II} and g factors ranging from 2 to 2.1. As observed in the previous SCM series[3] where Ni and Mn ions were bridged by the −NO− link, negative Weiss constants reveal dominant antiferromagnetic exchange between spin carriers. As seen in Figure 2, χT values at 300 K for **1**−**4** are 7.04, 6.87, 6.93, and 6.41 emu·K·mol^{-1}, respectively. With decreasing temperatures, χT continuously decreases to reach a minimum of 2.28 emu·K·mol^{-1} at 18 K for **1**, 2.24 emu·K·mol^{-1} at 20 K for **2**, 2.29 emu·K·mol^{-1} at 20 K for **3**, and 2.02 emu·K·mol^{-1} at 17 K for **4**, and then it slightly increases to reach a small peak (2.44 emu·K·mol^{-1} at 6.0 K for **1**, 2.42 emu·K·mol^{-1} at 5.6 K for **2**, 2.43 emu·K·mol^{-1} at 6.0 K for **3**, and 2.10 emu·K·mol^{-1} at 5.0 K for **4**) and finally decreases down to 1.82 K (2.15, 2.20, 2.19 and 2.04 emu·K·mol^{-1}, respectively, for **1**, **2**, **3**, and **4**).

As already demonstrated in the literature, the magnetic interactions between Mn^{III} ions via the bi-phenolate bridge, J_{Mn-Mn}, and between Mn^{III} and Ni^{II} via the −NO− bridge, J_{Mn-Ni}, are well-known to lead, respectively, to small ferromagnetic[3,10] and strong antiferromagnetic interactions.[3] To model this complex magnetic behavior, we have used a step-by-step approach. As a first stage, only strong J_{Mn-Ni} interactions have been considered. Therefore, from the $H = -2J_{Mn-Ni}S_{Mn}\cdot S_{Ni}$ spin Hamiltonian (where $S_{Mn} = 2$ and $S_{Ni} = 1$), the magnetic susceptibility of this $Mn^{III}-Ni^{II}$ dimer model can be derived at low field using the Van Vleck equation

$$\chi_{Ni-Mn} = \frac{Ng^2\mu_B^2}{kT}\frac{28\exp(10x) + 10\exp(4x) + 2}{7\exp(10x) + 5\exp(4x) + 3}$$

where $x = J_{Mn-Ni}/k_BT$. As shown Figure 2 for **1** (- - -), this model reproduces very well the high temperature regime and leads to reasonable J_{Ni-Mn} values ranging from −24 to −26 K along the series.[3] In the next step, the Mn···Mn interaction and also local anisotropy on the Mn^{III} and Ni^{II} ions must be considered to attempt a simulation of the whole temperature range. The consideration of all these parameters precludes a simple calculation of the tetramer's spin levels by Kambe's method;[11] hence, we have used a more general procedure developed by J. M. Clemente-Juan et al. (MAGPACK program).[12] Whereas the increasing χT product between 18 and 6 K (**1**) was modeled by considering J_{Mn-Mn}, its final decrease could not be reproduced taking into account only anisotropic effects with D_{Mn} ranging from −5 to 0 K and D_{Ni} ranging from −2 to 5 K (see Supporting Information). These results suggest that antiferromagnetic intermolecular interactions are necessarily relevant to describe this low temperature behavior. Therefore, the isotropic Heisenberg spin Hamiltonian for the tetramer unit, $H = -2J_{Mn-Ni}(S_{Mn(1)}\cdot S_{Ni(1)} + S_{Mn(1*)}\cdot S_{Ni(1*)}) - 2J_{Mn-Mn}(S_{Mn(1)}\cdot S_{Mn(1*)})$, has been used, and intertetramer magnetic interactions (zJ) have been treated in the frame of the mean-field approximation. The obtained best-sets of parameters for **1**−**4** are summarized in Table 2. As expected, values of J_{Ni-Mn} are found to be similar to those obtained with the Mn−Ni dimer model and in related materials.[3] Moreover, J_{Mn-Mn} interactions have been estimated to range from +0.4 to +0.9 K in good agreement with the values obtained for SCM[3] and Mn^{III} dimers.[10] These sets of magnetic interactions (Table 2) lead to $S = 2$ Ni_2Mn_2 tetramers which are antiferromagnetically interacting. A close analysis of the crystal packing shows that these intertetramer interactions may be mediated by π overlaps of bpy ligands. Indeed, it is worth noting that zJ values are probably overestimated as they also contain anisotropic contributions of the metal ions.[13]

In summary, a new series of heterometallic $Ni^{II}_2Mn^{III}_2$ tetramers, $[Mn(5\text{-R-saltmen})Ni(pao)(bpy)_2]_2(ClO_4)_4$, possessing an $S = 2$ spin ground state, have been synthesized by using the new $[Ni(pao)(bpy)_2]^+$ building block. The study of their magnetic properties confirms the local exchange obtained in the Mn_2Ni SCM series.

Acknowledgment. The authors would like to thank the Japan Science and Technology Agency (JST), the CNRS, the Université Bordeaux 1, and the Conseil Regional d'Aquitaine for financial support.

Supporting Information Available: X-ray data of **2**−**4** (CIF files) and χT versus T plots together with different fits for **1**−**4**. This material is available free of charge via the Internet at http://pubs.acs.org. CIF data (CCDC-237074 for **2**, 237075 for **3**, 237076 for **4**) available also on application to the Cambridge Data Centre, 12 Union Road, Cambridge CB21EZ, U.K. (Fax: (+44) 1223-336-033. E-mail: deposit@ccdc.cam.ac.uk).

IC049457Q

(10) Miyasaka, H.; Clérac, R.; Ishii, T.; Chang, H.; Kitagawa, S.; Yamashita, M. *J. Chem. Soc., Dalton Trans.* **2002**, 1528.
(11) Kambe, K. *J. Phys. Soc. Jpn* **1950**, *5*, 48.
(12) Borrás-Almenar, J. J.; Clemente-Juan, J. M.; Coronado, E.; Tsukerblat, B. S. *J. Comput. Chem.* **2001**, *22*, 985.
(13) It should be noted that magnetic simulations taking into account both intermolecular interaction and anisotropy of the metal ions are not reported here due to overparametrization and multiple solutions.